PHYSICAL REVIEW B **66**, 174437 (2002)

Low-frequency Raman modes of the single-molecule magnets Mn_{12}-acetate and Fe_8Br_8 and their analogs

J. M. North, R. M. Achey, and N. S. Dalal
Department of Chemistry and Biochemistry, and National High Magnetic Field Laboratory, Florida State University, Tallahassee, Florida 32306-4390

(Received 2 May 2002; revised manuscript received 5 July 2002; published 27 November 2002)

We report a 150–2000 cm^{-1} Raman study of the single-molecule magnets $Mn_{12}O_{12}$-acetate (Mn_{12}-Ac), deuterated Mn_{12}-Ac, Fe_8Br_8, O^{17}-labeled Fe_8Br_8, $Fe_8Br_{6.4}(ClO_4)_{1.6}$, and $Fe_8Br_4(ClO_4)_4$, all with a high-spin ground state of $S=10$. Raman spectra of Mn_8Fe_4, isostructural with Mn_{12}-Ac but with $S=2$, were essentially similar to those of Mn_{12}-Ac, thus ruling out the role of spin modes in this frequency range. The observed Raman modes at 287, 646, and 684 cm^{-1} are in reasonable agreement with the earlier reported density functional calculations of these modes and might thus be taken to support a proposed model of magnetic anisotropy of Mn_{12}-Ac. Raman modes of the Fe_8Br_8 system were assigned using small model compounds and measurements with polarized laser radiation, as well as ^{17}O isotopic labeling. Small but significant shifts in several mode frequencies have been detected in Fe_8Br_8 upon ClO_4^- substitution of Br^-, which might be helpful in future electronic structure calculations.

DOI: 10.1103/PhysRevB.66.174437 PACS number(s): 75.50.Xx, 78.20.Ls, 78.30.Jw

I. INTRODUCTION

This study describes a low-frequency (150-2000 cm^{-1}) Raman scattering investigation on compounds known as single-molecule magnets (SMM's), defined as systems where a magnetic domain can be reduced to a single molecule below a certain temperature known as the blocking temperature T_B.[1,2] The SMM's studied here are the two basic systems based on $[Mn_{12}O_{12}(CH_3COO)_{16}(H_2O)_4]\cdot 2\ CH_3COOH \cdot 4\ H_2O$,[3] abbreviated Mn_{12}-Ac, and $[(C_6H_{15}N_3)_6Fe_8(\mu_3\text{-}O)_2(\mu_2\text{-}OH)_{12}]Br_7(H_2O)Br\cdot 8H_2O$,[4] abbreviated Fe_8Br_8. The present study was prompted by the following observation. Mn_{12}-Ac was the first system that exhibited the phenomenon of the quantum tunneling of its magnetization (QTM),[5,6] which involves both phonon-assisted tunneling and pure quantum tunneling at lower temperatures. Although Mn_{12}-Ac has received considerable theoretical focus recently,[7–9] there is a scarcity of data on its phonon modes. An important step forward in this regard was the report by Sushkov *et al.*[10] of the infrared modes for Mn_{12}-Ac, some of which exhibited significant line shape changes under externally applied magnetic fields at liquid helium temperatures. Based partly on this observation, Pederson *et al.*[11] have carried out a density functional electronic structure calculation on Mn_{12}-Ac and have suggested that some specific low-frequency, Raman-active, Mn-O modes might be the origin of the so-called fourth-order magnetic anisotropy in Mn_{12}-Ac. The fourth-order anisotropy is the term $C(S_+^4+S_-^4)$ in the spin Hamiltonian for Mn_{12}-Ac,[2,12] where $S_\pm=S_x\pm iS_y$ are the usual spin operators. It contributes to $\Delta M_s=\pm 4$ transitions involved in the mechanism of the phonon-assisted tunneling of the magnetization in the system. It was thus of interest to measure the Raman modes of Mn_{12}-Ac (Ref. 13) and then to extend the studies to Fe_8Br_8 as well.

As additional background, we note that SMM's have been of high interest lately for several reasons. First, they hold the promise of leading to memory storage devices at molecular dimensions.[1,2] Second, as stated above, they exhibit the QTM phenomenon whose origin is still not fully understood. QTM was first observed in Mn_{12}-Ac (Refs. 5 and 6) and later in Fe_8Br_8.[14] The most studied of the SMM's is still Mn_{12}-Ac. As shown in Fig. 1, the core of Mn_{12}-Ac consists of 12 mixed-valence Mn ions: eight $Mn^{3+}(3d^4,S=2)$ in a crown, coupled ferromagnetically to yield a $S=16$ state, and four Mn^{4+} $(3d^3,S=3/2)$ arranged in a cubane structure which are also coupled ferromagnetically for a total of $S=6$. These two subsystems are antiferromagnetically coupled to give rise to a net total spin of $S=16-6=10$.[2] Fe_8Br_8, as shown in Fig. 2, consists of eight high-spin Fe^{3+} $(S=5/2)$ ions. Six are coupled ferromagnetically and the two remaining Fe^{3+} interact antiferromagnetically with

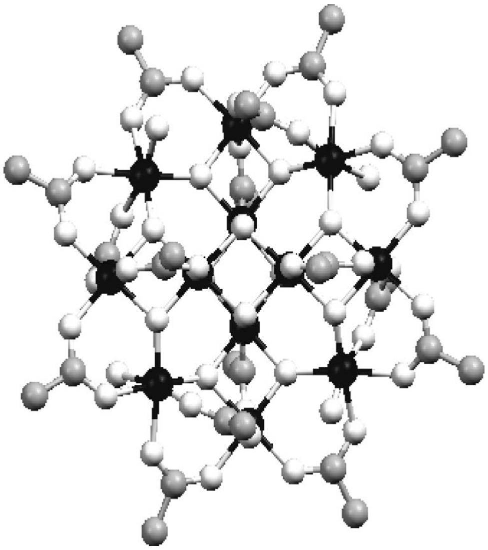

FIG. 1. Structure of Mn_{12}-Ac with acetate ligand. Black = Mn, white = O, and gray = C. The H_2O molecules are omitted for clarity (Ref. 3).

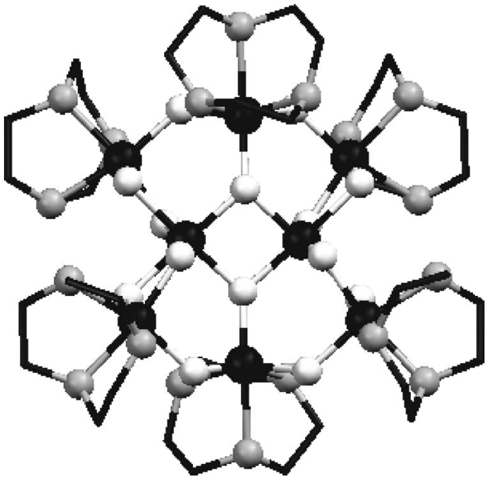

FIG. 2. Structure of Fe_8Br_8 showing the 1,4,7 triazacyclononane ligand. Black circles = Fe, white circles = O, gray circles = N, and black rods = C. The Br atoms are omitted for clarity (Ref. 4).

those six, for a net total spin of $S=10$ as well. It should be noted that in both cases the ordered single-molecule magnetic domains are not present at room temperature, but only below their blocking temperature T_B, which is about 3 K for Mn_{12}-Ac and 1 K for Fe_8Br_8.[5,6,15,16] These systems can be visualized in the spin space as being in a double-minimum potential in a zero external field, the levels being doubly degenerate in the $+/-M_s$ spin-quantum numbers where M_s takes the usual $(2S+1)$ values $-S,-S+1,\ldots+S$. QTM is defined as the phenomenon of the tunneling of the magnetization vector from the levels in one well (labeled $-M_s$) to those in the other well (labeled $+M_s$).[1] The spin-energy levels in Mn_{12}-Ac and Fe_8Br_8 have been characterized by magnetization,[5,6,14,15] zero-field electron paramagnetic resonance (EPR),[16–18] high-field EPR,[19–21] neutron scattering,[22,23] excited-state EPR and relaxation,[24] EPR line broadening,[25] micro-Hall measurements,[26] torque magnetometry,[15,27] infrared absorption under magnetic field,[10] optical spectroscopy,[28] dielectric relaxation,[29] NMR spectroscopy,[30–36] and specific heat measurements.[37–39] There has also been a parallel theoretical effort,[7–9,11,12,40–43] but a quantitative mechanism of QTM still remains controversial. No previous Raman measurements are available on these systems, except for a preliminary recent report on Mn_{12}-Ac from our laboratory.[13]

The paper is organized as follows. Experimental details of this study are provided in Sec. II. Section III A contains the results and discussion on Mn_{12}-Ac, while Sec. III B describes those on Fe_8Br_8. The conclusions are summarized in Sec. IV.

II. EXPERIMENT

A. Sample synthesis and crystal growth

High-quality single crystals of Mn_{12}-Ac were synthesized as described by Lis.[3] Deuterated Mn_{12}-Ac was prepared from CD_3COOD and D_2O, under a nitrogen atmosphere. Mn_8Fe_4 (Fig. 3) was prepared following the procedure of Schake *et al.*[44] by mixing $Fe(CH_3CO_2)_2$ and $KMnO_4$. The crystals grew as rectangular rods with prismatic ends, with the easy magnetization axis being along the longest direction. The size of a single crystal used was typically $0.6\times0.6\times2.8$ mm^3. Single crystals of Fe_8Br_8 were synthesized following the method of Wieghardt *et al.*[4] ^{17}O-labeled Fe_8Br_8 was prepared from ^{17}O-enriched H_2O. Samples containing 20% and 50% perchlorate $(ClO_4{}^-)$ were synthesized by the substitution of the appropriate molar ratio of perchlorate for bromide in the method of Wieghardt *et al.*[4] They were identified as $Fe_8Br_{6.4}(ClO_4)_{1.6}$ and $Fe_8Br_4(ClO_4)_4$. The samples were characterized by NMR, x-ray diffraction, and magnetization measurements. $FeCl_3$tacn (tacn = 1,4,7 triazacyclononane) was also synthesized as described earlier.[4] The smaller model compounds Fe_2O_3, tacn, and $NaClO_4$ were of commercial grade.

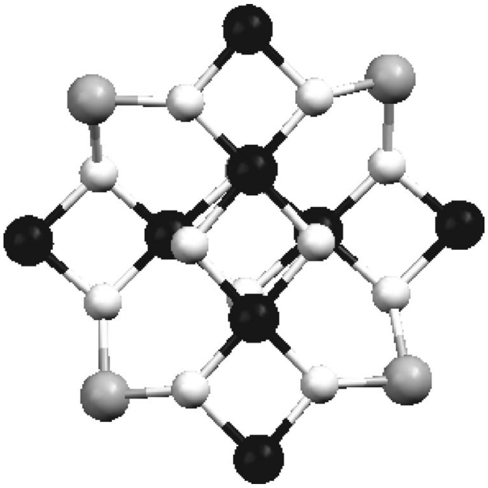

FIG. 3. Core structure of Mn_8Fe_4. Black = Mn, white = O, and gray = Fe. The acetate has been omitted (Ref. 44).

B. Raman measurements

Raman spectra were collected using a microRaman spectrograph, the JY Horiba LabRam HR800, excited by a TUIOptics laser emitting 80 mW of power at 785 nm. A low-power objective, 5×0.10 NA, maximized the exposed sample area, and long exposure times (2400 sec) were used to collect sufficient signal with four scans per spectrum for Mn_{12}-Ac. The Fe_8Br_8 spectra were acquired under slightly different conditions. A 0.6 o.d. neutral density filter in conjunction with shorter collection times (480 sec) was used in order to obtain a sufficient signal with four scans per spectrum.

A noteworthy point is that the crystals are highly susceptible to laser damage. Under full laser power, the Raman spectra changed from the usual large number of sharp peaks to much fewer and broad signals. The broad peaks were irreversible on reducing the laser power or with time over several days as seen in Fig. 4. Care must be taken to optimize the laser power for the best resolution

III. RESULTS AND DISCUSSION

Our Raman measurements focused on the 150–2000 cm^{-1} range partly because of our experimental

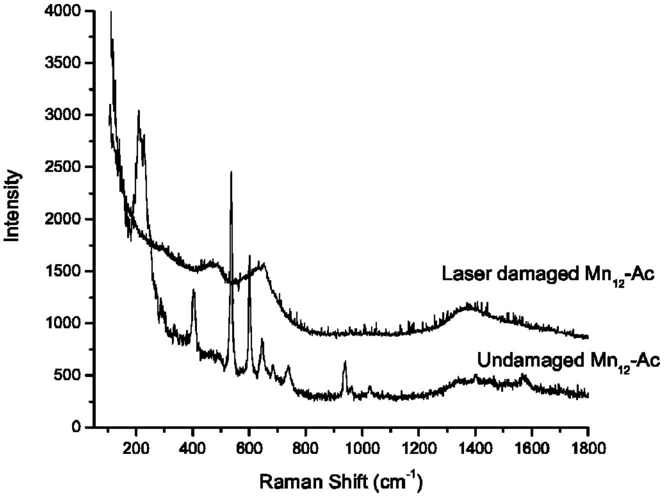

FIG. 4. Raman spectra of laser-damaged Mn_{12}-Ac and undamaged Mn_{12}-Ac.

limitations and partly because of the theoretical prediction by Pederson *et al.*[11] that the modes in this range would be particularly relevant to the QTM phenomenon.

A. Mn_{12}-Ac and analogs

In Fig. 5, a typical Raman spectrum of Mn_{12}-Ac is shown in comparison to its analogs. The spectra are very similar to one another and consist of several sharp peaks. The spectrum of Mn_8Fe_4,[44] with $S=2$, compares well with the spectrum of $S=10$ Mn_{12}-Ac. Because iron is only one atomic mass unit higher than manganese, the Mn_8Fe_4 modes can be expected to show only small isotopic shifts. Similar conclusions can be drawn regarding the spectrum of the deuterated Mn_{12}-Ac. Again, due to the relative size of the cluster as compared to the slight mass increase due to the replacement of hydrogen with deuterium, only a very small difference can be noted. It should be noted that Raman spectroscopy gives a fingerprint of Mn_{12}-Ac, thus showing its potential as an analytical technique for the identification of SMM analogs. Further mode analysis of Mn_{12}-Ac was accomplished by using model compounds such as $KMnO_4$ and Mn_3O_4 as reported earlier.[13] The mode assignments are presented in Table I, together with the theoretical estimates by Pederson *et al.*[11]

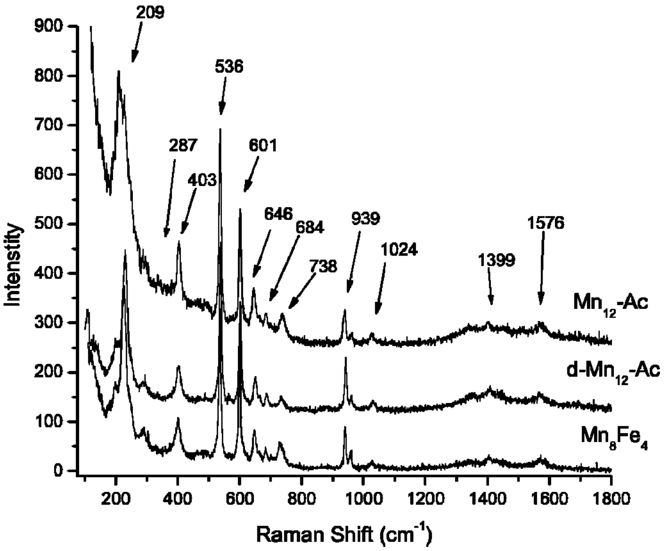

FIG. 5. Raman spectra of Mn_{12}-Ac, deuterated Mn_{12}-Ac, and isostructural, $S=2$, Mn_8Fe_4. The numbers with the arrows are the mode frequencies in cm^{-1}.

TABLE I. Raman modes (cm^{-1}) and theoretical calculations of (Ref. 11) of vibrational modes for Mn_{12}-Ac.

Mn_{12}-Ac	d-Mn_{12}-Ac	Mn_8Fe_4	Theory	Assignment
209	229	227	270	Mn-O
287	293	290	281	Mn-O
403	403	401		Mn-O
536	537	538	465	Mn-O
601	601	601		Mn-O
646	650	650	630	Mn-O
684	687	684	670	Mn-O
738	734	731		
939	944	945		Mn-acetate
1024	1028	1028		Symmetric C-O stretch
1399	1409	1402	1496	Acetate stretch
1576	1574	1574		Asymmetric C-O stretch

A review of the observed IR modes[10] shows several similarities as compared with the Raman data. As noted by Sushkov *et al.* several of the observed infrared bands display noticeable spectral broadening under externally applied magnetic fields.[10] This result suggests that these and perhaps other infrared bands involve interactions with the magnetic moment. Pederson *et al.*[11] cite this observation as the basis for their proposal that low-frequency Mn-O vibrations such as the 284 and 408 cm^{-1} infrared modes play an important role in rendering the fourth-order magnetic anisotropy to the Mn_{12}-Ac-based SMM's. Hence they could be thought of as playing a significant role in the mechanism of QTM in this system. Similar Raman modes observed at 287 and 403 cm^{-1} should also exhibit line shape changes under an externally applied magnetic field. Such studies (under progress) should provide additional help in the characterization of these modes and the understanding of the QTM phenomenon in the Mn_{12}-Ac SMM's.

B. Fe_8Br_8 and analogs

Figure 6 shows the Raman spectra for Fe_8Br_8 and its ^{17}O-labeled analog. The measured mode frequencies are presented in Table II. The bands are comparable in intensity and shape for the two lattices. Because of the small effect of isotopic substitution on the overall mass of the cluster, there is only a very small isotopic shift in the peak values, as may be noted from Table II. Nevertheless, the similarity of the observations lends support to the authenticity of the lattices and, conversely, to the band assignment. As for Mn_{12}-Ac,[13] the complexity of the Fe_8Br_8 structure and the lack of symmetry prevented us from carrying out a formal group theoretical analysis. Also, there are no electronic structure calcu-

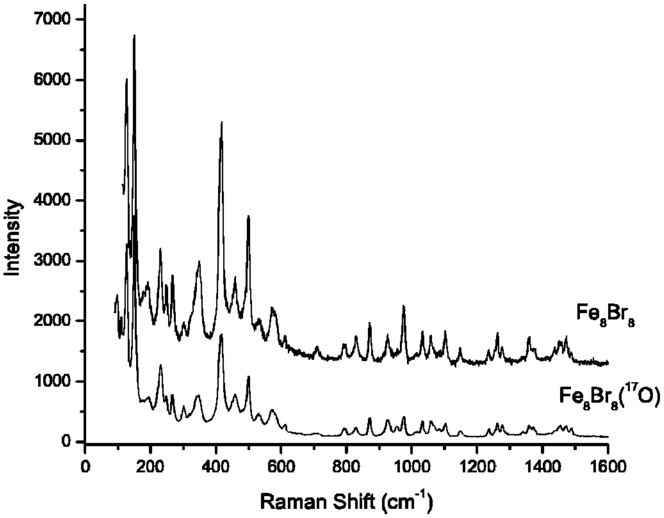

FIG. 6. Raman spectra of Fe_8Br_8, and ^{17}O-labeled Fe_8Br_8.

lations available for this system. We thus again resorted to the use of model compounds for the mode assignment.

The compounds with 20% and 50% perchlorate (ClO_4^-) substitution, $Fe_8Br_{6.4}(ClO_4)_{1.6}$ and $Fe_8Br_4(ClO_4)_4$, respectively, exhibited several small perturbations throughout the entire spectrum in comparison to Fe_8Br_8, as may be noted from Fig. 7. Many of the peaks are of similar size, shape, and intensity, but shifted to slightly different frequencies. An ex-

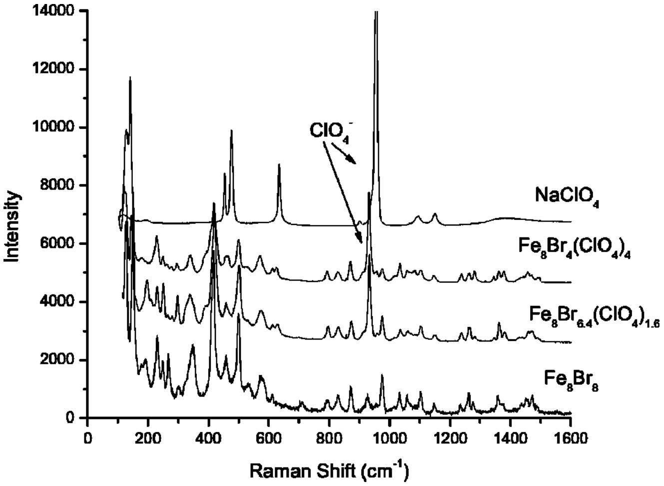

FIG. 7. Raman spectra of Fe_8Br_8, perchlorate analogs, and $NaClO_4$.

TABLE II. Raman modes and assignments of Fe_8Br_8 and analogs (cm^{-1}). w=weak, s=strong.

Fe_8Br_8	Fe_8Br_8 (^{17}O)	$Fe_8Br_{6.4}(ClO_4)_{1.6}$	$Fe_8Br_4(ClO_4)_4$	Assignment
127	127	119	127	Fe-N
151	150	144	141	Fe-N
191	194	197	179	tacn
230	231	230	229	Fe-O
250	248	250	249	Fe-O and Fe-N
268	267	266(w)	263(w)	
301	301	299	296	Fe-O and Fe-N
348	348	341	341	tacn
417	416	419	419	Fe-O and Fe-N
459	459	458	463	
499	501	501	500	Fe-O and Fe-N
533	531	528	527	tacn
575	573	573	571	tacn
611	612	613	612	Fe-O
709	709	629	626	
794	794	795	793	tacn
829	828	829	829	tacn
870	871	873	870	tacn
926	927	933(s)	933(s)	933 ClO_4^-
974	975	975	975	tacn
1033	1033	1035	1034	tacn
1059	1058	1060	1057	tacn
1102	1103	1103	1103	tacn
1148	1149	1148	1147	tacn
1235	1236	1237	1239	tacn
1263	1263	1264	1264	tacn
1277	1277	1283	1281	tacn
1358	1358	1363	1362	tacn
1375	1373	1381	1379	tacn
1474	1472	1472	1471	tacn

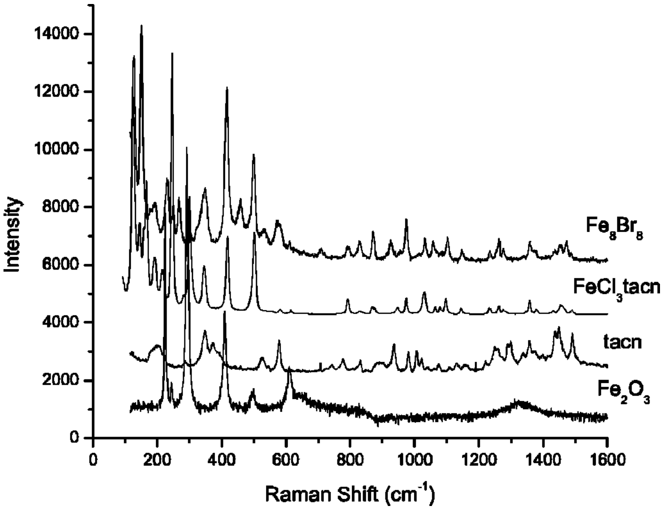

FIG. 8. Raman spectrum of Fe_8Br_8 shown in comparison to spectra of compounds $FeCl_3$tacn, tacn, and Fe_2O_3.

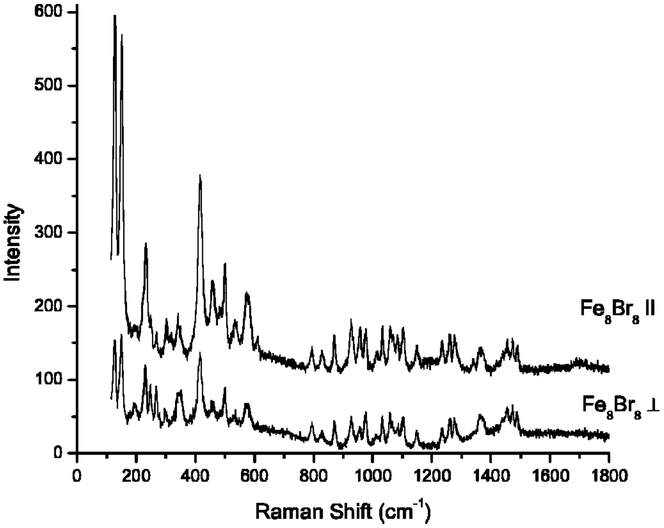

FIG. 9. Polarized Raman spectra of Fe_8Br_8.

ample of this is seen with the mode observed at 151 cm^{-1} in Fe_8Br_8 as compared with the peak at 141 cm^{-1} in the $Fe_8Br_4(ClO_4)_4$. This mode is assigned as an Fe-N stretch based upon its absence in $NaClO_4$, Fe_2O_3, and tacn, but presence in $FeCl_3$tacn (Fig. 7). A comparison of the data for the perchlorate derivatives with $NaClO_4$ reveals the modes which can be assigned to perchlorate vibrations. The sharp, strong peaks at 933 cm^{-1} in the perchlorate analogs are only slightly shifted from the sharp totally symmetric (*A*) vibration at 956 cm^{-1}. The peaks at 933 cm^{-1} are indicative of ionic perchlorate in the cluster.[45] The relative intensity of the peak at 933 cm^{-1} increases with the higher percentage of perchlorate in the molecule. A comparison of the peak positions and assignments is provided in Table II.

The spectra from 1,4,7 triazacyclononane (tacn), $FeCl_3$tacn, and Fe_2O_3 (Fig. 8) helped in the assignments for the ligands in Fe_8Br_8. First, a comparison of the spectra of $FeCl_3$tacn, tacn, and Fe_8Br_8 (Fig. 8) shows that most of the peaks above 800 cm^{-1} are due mostly to vibrations in the organic ligand, tacn. Second, the peak observed at 575 cm^{-1} for Fe_8Br_8 is also evident for $FeCl_3$tacn and tacn at 578 cm^{-1}, thus assignable to the ligand, as also that at 348 cm^{-1} in Fe_8Br_8. The peak at 193 cm^{-1} in Fe_8Br_8 is also observed in $FeCl_3$tacn and can thus be assigned as an Fe-N stretch. The mode at 500 cm^{-1} in Fe_8Br_8 appears to be a superposition of the peak at 502 cm^{-1} in $FeCl_3$tacn and the A_{1g} (Ref. 46) peak at 498 cm^{-1} in Fe_2O_3. This is also the case for the peak in Fe_8Br_8 at the observed frequency of 417 cm^{-1}. Because oxygen is only slightly heavier than nitrogen, it is not surprising that the Fe-N and Fe-O stretches occur at very close frequencies in $FeCl_3$tacn and Fe_2O_3. For this reason we have assigned the peaks at 417 and 500 cm^{-1} to a superposition of Fe-N and Fe-O stretches.

As seen in Fig. 9, Raman spectra were collected parallel and perpendicular to the incident radiation. The polarized anisotropy was examined to assign the various stretches as symmetric and antisymmetric. When the scattering is polarized parallel to the incident light it is possible to see all of the peaks. When the scattering is polarized perpendicular to the incident light, the symmetric peaks are of lower relative intensity. Through these studies we have assigned the two intense peaks at 127 and 151 cm^{-1} as symmetric stretches. The three peaks at 417, 459, and 499 cm^{-1} are also assigned as a symmetric stretches. Most of the peaks in the ligand correspond to asymmetric stretches with the exception of peaks at 955 and 1341 cm^{-1}, which are assigned as symmetric stretches.

Preliminary temperature dependence experiments on Fe_8Br_8 from 300 to 78 K have shown some slight shifts in some of the low-frequency Raman modes (Fig. 10). The mode observed at 151 cm^{-1} shifts to the slightly higher frequency of 154 cm^{-1}. However it is interesting to note that the peak seen at 127 cm^{-1} stays relatively constant, seeming to be relatively temperature independent. This provides further evidence that the mode at 151 cm^{-1} can be attributed to an Fe-N vibration. It makes sense that the Fe-N bonds to the

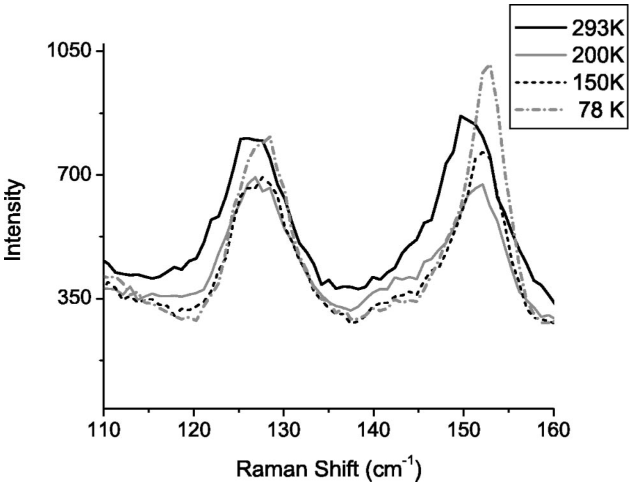

FIG. 10. Temperature dependence on the low-frequency Raman modes of Fe_8Br_8.

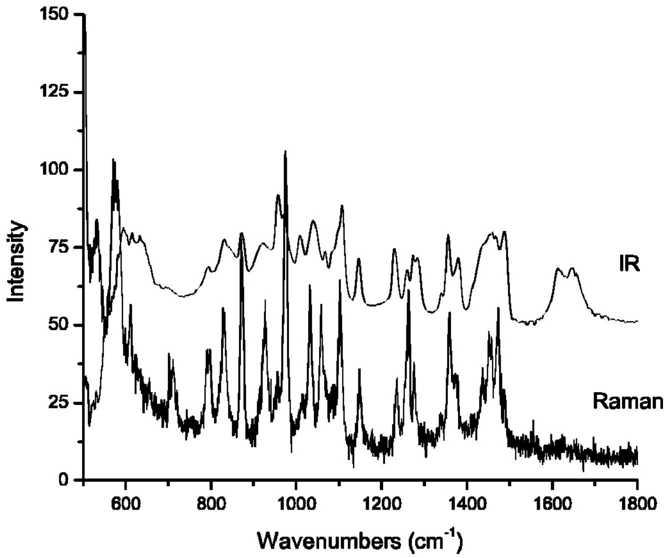

FIG. 11. Infrared and Raman spectra of Fe_8Br_8.

tacn ligand would be more affected than the Fe-O bonds in the core of the cluster. It is anticipated that further experiments below 77 K will give rise to more spectral changes, as we approach the blocking temperature.

A comparison of the Raman and infrared spectra of Fe_8Br_8 (Fig. 11) shows many comparable modes. The size and shape of several of the peaks correspond well between the two techniques. For example, the Raman peaks at 1358 and 1375 cm^{-1} are almost identically reproduced in the infrared data at 1357 and 1379 cm^{-1}. Higher resolution infrared studies under the influence of externally applied magnetic field as done for Mn_{12}-Ac,[10] together with electronic structure calculations, are needed for a further understanding of the nature of these modes in the Fe_8Br_8 system.

IV. CONCLUSIONS

By using near-infrared laser excitation and, systematically suppressing diffuse scattering and laser damage, we have succeeded in obtaining the first Raman spectra of the single-molecule magnets Mn_{12}-Ac, Fe_8Br_8, and their analogs. While the high structural complexity of these large molecules has prevented us from carrying out detailed group theoretical analysis of the modes, we were able to make their assignments by using the spectra of the constituent small model compounds. For Mn_{12}-Ac, the spin effects were largely delineated by comparison with the isostructural $S = 2$ analog Mn_8Fe_4. We note that there will be some common spin modes between the $S = 2$ and $S = 10$ systems, but those will be at frequencies much too small for Raman measurements. Good agreement has been found between our observed spectra for the Mn-O modes with the recent density functional electronic structural calculation of Pederson *et al.*[11] This agreement could be taken as a possible support for the proposal[11] that the deformation resulting from these modes might contribute to the magnetic anisotropy of Mn_{12}-Ac.

The present report of the vibrational data on the Fe_8Br_8 analogs should elicit additional experimental and theoretical studies and thereby lead to further understanding of this system as well. Finally, we note that Raman measurements constitute an easy fingerprint of these SMM's, especially of the effects of ligand substitutions as in the $Fe_8Br_{8-x}(ClO_4)_x$ family.

ACKNOWLEDGMENTS

We thank the National Science Foundation (NIRT Grant No. DMR 0103290) for financial support. We would like to thank Dr. Bert van de Burgt for help with the Raman measurements and Dr. Khalil A. Abboud for x-ray characterizations.

---

[1] D.D. Awschalom, D.P. Di Vincenzo, and J.F. Smyth, Science **258**, 414 (1992).

[2] E. M. Chudnovsky and J. Tejada, *Macroscopic Quantum Tunneling of the Magnetic Moment* (Cambridge University Press, Cambridge, England, 1998).

[3] T. Lis, Acta Crystallogr., Sect. B: Struct. Crystallogr. Cryst. Chem. **36**, 2042 (1980).

[4] K. Weighardt, K. Pohl, I. Jibril, and G. Huttner, Angew. Chem. Int. Ed. Engl. **23**, 77 (1984).

[5] J.R. Friedman, M.P. Sarachik, J. Tejada, and R. Ziolo, Phys. Rev. Lett. **76**, 3830 (1996).

[6] L. Thomas, F. Lionti, R. Ballou, D. Gatteschi, R. Sessoli, and B. Barbara, Nature (London) **383**, 145 (1996).

[7] M.N. Leuenberger and D. Loss, Phys. Rev. B **61**, 1286 (2000).

[8] D.A. Garanin and E.M. Chudnovsky, Phys. Rev. B **56**, 11 102 (1997).

[9] E.M. Chudnovsky and D.A. Garanin, Phys. Rev. Lett. **87**, 187203 (2001).

[10] A.B. Sushkov, B. Jones, J.L. Musfeldt, R.M. Achey, and N.S. Dalal, Phys. Rev. B **63**, 212408 (2001).

[11] M.R. Pederson, N. Bernstein, and J. Kortus, Phys. Rev. Lett. **89**, 097202 (2002).

[12] P. Politi, A. Rettori, F. Hartmann-Boutron, and J. Villain, Phys. Rev. Lett. **75**, 537 (1995).

[13] J.M. North, L.J. van de Burgt, and N.S. Dalal, Solid State Commun. **123**, 75 (2002).

[14] C. Sangregorio, T. Ohm, C. Paulsen, R. Sessoli, and D. Gatteschi, Phys. Rev. Lett. **78**, 4645 (1997).

[15] J.A.A.J. Perenboom, J.S. Brooks, S. Hill, T. Hathaway, and N.S. Dalal, Phys. Rev. B **58**, 330 (1998).

[16] A. Mukhin, V.D. Travkin, A.K. Zvezdin, S.P. Lebedev, A. Caneschi, and D. Gatteschi, Europhys. Lett. **44**, 778 (1998).

[17] A. Mukhin, B. Gorshunov, M. Dressel, C. Sangregorio, and D. Gatteschi, Phys. Rev. B **63**, 214411 (2001).

[18] M. Dressel, B. Gorshunov, K. Rajagopal, S. Vongtragool, and A.A. Mukhin, cond-mat/0110340v2 (unpublished).

[19] A.L. Barra, D. Gatteschi, and R. Sessoli, Phys. Rev. B **56**, 8192 (1997).

[20] S. Hill, J.A.A.J. Perenboom, N.S. Dalal, T. Hathaway, T. Stalcup, and J.S. Brooks, Phys. Rev. Lett. **80**, 2453 (1998).

[21] S. Hill, S. Maccagnano, K. Park, R.M. Achey, J.M. North, and N.S. Dalal, Phys. Rev. B **65**, 224410 (2002).

[22] M. Hennion, L. Pardi, I. Mirebeau, E. Suard, R. Sessoli, and A. Caneschi, Phys. Rev. B **56**, 8819 (1997).

[23] I. Mirebeau, M. Hennion, H. Casalta, H. Anders, H.U. Gudel, A.V. Ivadova, and A. Caneschi, Phys. Rev. Lett. **83**, 628 (1999).

[24] R. Blinc, P. Cevc, D. Arcon, N.S. Dalal, and R.M. Achey, Phys. Rev. B **63**, 212401 (2001).

[25] K. Park, M.A. Novotny, N.S. Dalal, S. Hill, and P.A. Rikvold, Phys. Rev. B **65**, 014426 (2001); J. Appl. Phys. **91**, 7167 (2002).

[26] L. Bokacheva, A.D. Kent, and M.A. Walters, Phys. Rev. Lett. **85**, 4803 (2000); K.M. Mertes, Y. Suzuki, M.P. Sarchik, Y. Paltiel, H. Shtrikman, E. Zeldov, E.M. Rumberger, D.N. Hendrickson, and G. Christou, Phys. Rev. B **65**, 212401 (2002).

[27] I. Chiorescu, R. Girraud, A.G.M. Jansen, A. Caneschi, and B. Barbara, Phys. Rev. Lett. **85**, 4807 (2000).

[28] S.M. Oppenheimer, A.B. Sushkov, J.L. Musfeldt, R.M. Achey, and N.S. Dalal, Phys. Rev. B **65**, 054419 (2002).

[29] Z. Kutnjak, G. Filipic, L. Levstik, R.M. Achey, and N.S. Dalal, Phys. Rev. B **59**, 11 147 (1999).

[30] A. Lascialfari, Z.H. Jang, F. Borsa, P. Carretta, and D. Gatteschi, Phys. Rev. Lett. **81**, 3773 (1998).

[31] Y. Furukawa, K. Watanabe, K. Kumagai, Z.H. Jang, A. Lascialfari, F. Borsa, and D. Gatteschi, Phys. Rev. B **62**, 14 246 (2000).

[32] D. Arcon, J. Dolinsek, T. Apih, R. Blinc, N.S. Dalal, and R.M. Achey, Phys. Rev. B **58**, 2941 (1998); J. Dolinsek, D. Arcon, R. Blinc, P. Vonlanthen, H.R. Ott, R.M. Achey, and N.S. Dalal, Europhys. Lett. **42**, 691 (1998).

[33] R.M. Achey, P. Kuhns, A. Reyes, W. Moulton, and N.S. Dalal, Polyhedron **20**, 1745 (2001); Phys. Rev. B **64**, 064420 (2001); Solid State Commun. **121**, 107 (2002).

[34] T. Goto, T. Kudo, T. Koshida, Y. Fujii, A. Oyamada, J. Arai, K. Takeda, and K. Awaga, Physica B **1227**, 284 (2000).

[35] Y. Furukawa, K. Watanabe, K. Kumagai, F. Borsa, and D. Gatteschi, Phys. Rev. B **64**, 104401 (2001).

[36] T. Kubo, T. Goto, T. Koshiba, K. Takeda, and K. Awaga, Phys. Rev. B **65**, 224425 (2002).

[37] A.M. Gomes, M.A. Novak, R. Sessoli, A. Caneschi, and D. Gatteschi, Phys. Rev. B **57**, 5021 (1998).

[38] F. Fominaya, J. Villain, P. Gandit, J. Chaussy, and A. Caneschi, Phys. Rev. Lett. **79**, 1126 (1997).

[39] M. Sales, J.M. Hernandez, J. Tejada, and J.L. Martinez, Phys. Rev. B **60**, 14 557 (1999).

[40] F. Luis, J. Bartlome’, and J.F. Fernandez, Phys. Rev. B **57**, 505 (1998).

[41] J.F. Fernandez, cond-mat/0110540 v1 (unpublished).

[42] A.K. Zvezdin, V.V. Dobrovitski, B.N. Harmon, and M.I. Katsnelson, Phys. Rev. B **58**, 14 733 (1998).

[43] H.A. De Raedt, A.H. Hams, V.V. Dobrovitski, M. Al-Saqer, M.I. Katsnelson, and B.N. Harmon, J. Magn. Magn. Mater. **246**, 392 (2002).

[44] A.R. Schake, H. Tsai, R.J. Webb, K. Folting, G. Christou, and D.N. Hendrickson, Inorg. Chem. **33**, 6020 (1994).

[45] K. Nakamoto, *Infrared and Raman Spectra of Inorganic and Coordination Compounds* (Wiley Interscience, New York, 1997), Pt. B, pp. 59–62 and 82.

[46] L.F.C. de Oliveira, H.G.M. Edwards, R.L. Frost, J.T. Kloprogge, and P.S. Middleton, Analyst (Cambridge, U.K.) **127**, 536 (2002).